Mode-cleaning and injection optics of the gravitational-wave detector GEO600

S. Goßler[a)]
Universität Hannover, Institut für Atom- und Molekülphysik, Abteilung Spektroskopie, Callinstrasse 38, D-30167 Hannover, Germany

M. M. Casey
Department of Physics and Astronomy, University of Glasgow, Glaskow G12 8QQ, United Kingdom

A. Freise
Universität Hannover, Institut für Atom- und Molekülphysik, Abteilung Spektroskopie, Callinstrasse 38, D-30167 Hannover, Germany

A. Grant
Department of Physics and Astronomy, University of Glasgow, Glaskow G12 8QQ, United Kingdom

H. Grote
Universität Hannover, Institut für Atom- und Molekülphysik, Abteilung Spektroskopie, Callinstrasse 38, D-30167 Hannover, Germany

G. Heinzel
Max-Planck-Institut für Gravitationsphysik, Albert-Einstein-Institut, Teilinstitut Hannover, Callinstrasse 38, D-30167 Hannover, Germany

M. Heurs
Universität Hannover, Institut für Atom- und Molekülphysik, Abteilung Spektroskopie, Callinstrasse 38, D-30167 Hannover, Germany

M. E. Husman
Department of Physics and Astronomy, University of Glasgow, Glaskow G12 8QQ, United Kingdom

K. Kötter, V. Leonhardt, H. Lück,[b)] and M. Malec
Universität Hannover, Institut für Atom- und Molekülphysik, Abteilung Spektroskopie, Callinstrasse 38, D-30167 Hannover, Germany

K. Mossavi
Max-Planck-Institut für Gravitationsphysik, Albert-Einstein-Institut, Teilinstitut Hannover, Callinstrasse 38, D-30167 Hannover, Germany

S. Nagano
TAMA Project, National Astronomical Observatory, Mitaka, Tokyo 181-8588, Japan

P. W. McNamara and M. V. Plissi
Department of Physics and Astronomy, University of Glasgow, Glaskow G12 8QQ, United Kingdom

V. Quetschke
Universität Hannover, Institut für Atom- und Molekülphysik, Abteilung Spektroskopie, Callinstrasse 38, D-30167 Hannover, Germany

D. I. Robertson and N. A. Robertson[c)]
Department of Physics and Astronomy, University of Glasgow, Glaskow G12 8QQ, United Kingdom

A. Rüdiger and R. Schilling
Max-Planck-Institut für Gravitationsphysik, Albert-Einstein-Institut, Hans-Kopfermann-Straße 1, D-85748 Garching, Germany

K. D. Skeldon, K. A. Strain, C. I. Torrie,[d)] and H. Ward
Department of Physics and Astronomy, University of Glasgow, Glaskow G12 8QQ, United Kingdom

U. Weiland and B. Willke
Universität Hannover, Institut für Atom- und Molekülphysik, Abteilung Spektroskopie, Callinstrasse 38, D-30167 Hannover, Germany

W. Winkler
Max-Planck-Institut für Gravitationsphysik, Albert-Einstein-Institut, Hans-Kopfermann-Straße 1, D-85748 Garching, Germany

J. Hough
Department of Physics and Astronomy, University of Glasgow, Glaskow G12 8QQ, United Kingdom

0034-6748/2003/74(8)/3787/9/$20.00

K. Danzmann[b)]
Universität Hannover, Institut für Atom- und Molekülphysik, Abteilung Spektroskopie, Callinstrasse 38, D-30167 Hannover, Germany

(Received 29 January 2003; accepted 6 May 2003)

The British–German interferometric gravitational-wave detector GEO600 uses two high-finesse triangular ring cavities of 8 m optical pathlength each, as an optical mode-cleaning system. The modecleaner system is housed in an ultrahigh-vacuum environment to avoid contamination of the optics and to minimize both the influence of refractive index variations of the air and acoustic coupling to the optics. To isolate the cavities from seismic noise, all optical components are suspended as double pendulums. These pendulums are damped at their resonance frequencies at the upper pendulum stage with magnet-coil actuators. A suspended reaction mass supports three coils matching magnets bonded onto the surface of one mirror of each cavity, allowing length control of the modecleaner cavities to maintain resonance with the laser light. A fully automated control system stabilizes the frequency of the slave laser to that of the master laser, the frequency of the master laser to the length of the first modecleaner and the length of the first to the length of the second modecleaner. The control system uses the Pound–Drever–Hall sideband technique and operates autonomously over long time periods with only infrequent human interaction. The duty cycle of the system was measured to be 99.7% during an 18 day period. The throughput of the whole modecleaner system is about 50%. In this article, we give an overview of the mechanical and optical setup and the achieved performance of the double modecleaner system. © *2003 American Institute of Physics.* [DOI: 10.1063/1.1589160]

I. INTRODUCTION

The direct detection and analysis of gravitational waves emitted by astronomical sources is very likely to give a much better understanding of the existing universe.[1–3] The interferometric approach to the detection of gravitational waves yields, in contrast to the resonant mass detectors,[4] a much broader detection bandwidth from several tens of Hz to a few kHz. Worldwide four earth-bound interferometric gravitational-wave detector projects are currently under construction: The LIGO project in the USA with two detectors of 4 km length each and a third one with a length of 2 km,[5] the French–Italian VIRGO collaboration with an interferometer of 3 km arm length,[6] the 300 m TAMA300 project in Japan,[7] and the British-German GEO600 detector near Hannover, Germany.[8–10]

GEO600 is a dual-recycled Michelson interferometer with arms of 1200 m length, each folded once. The nominal operating point of the interferometer is the so-called ''dark fringe'' at which, ideally, all of the light is reflected back to the input port. The technique of power recycling allows maximization of the light power stored in the Michelson interferometer by placing a mirror in the input port of the interferometer (see Fig. 1). Placing a further mirror in the output port provides an enhancement of the phase modulation sidebands induced by gravitational waves. With this technique of signal recycling, the frequency response of the interferometer becomes adjustable by changing the reflectivity of the signal recycling mirror (and/or position).[11]

In order to achieve the GEO600 strain sensitivity goal of $h \simeq 5\times10^{-22}/\sqrt{\mathrm{Hz}}$ at 100 Hz, the illuminating laser light is required to be very stable in power, frequency, and geometry. Hence, it is filtered temporally and spatially by a sequential two-cavity modecleaner system. Since the modecleaner system needs to be seismically isolated, we have suspended all its optical components and chose double pendulums to accomplish this.

The main optical components of the interferometer itself are suspended as triple cascaded pendulums to provide even greater seismic isolation for these more sensitive optics. Each double and triple suspension is actively damped at its first (uppermost) stage, using position sensors with feedback to magnet-coil actuators, to suppress the excessive motion at its resonances.[12,13]

In the following, the need for a double modecleaner system for GEO600 will be deduced from the required spatial and temporal stability. Then, a description of the optical and mechanical setup and finally the achieved performance and reliability of the system will be given.

II. DESIGN REQUIREMENTS

For simplicity, the effects due to signal recycling (e.g., mode healing)[11] are neglected in the following calculations and hence the interferometer is treated as a power-recycled Michelson interferometer. Thus, the results derived can be considered those of a ''worst case,'' and the real requirements would be more relaxed.

The error signal needed to keep the interferometer on the dark fringe is obtained using a technique known as Schnupp (or ''frontal'') modulation which requires slightly different arm lengths of the interferometer. As a result, the laser fre-

a)Author to whom correspondence should be addressed; electronic mail: sfg@mpq.mpg.de
b)Max-Planck-Institut für Gravitationsphysik, Albert-Einstein-Institut, Teilinstitut Hannover, Callinstrasse 38, D-30167 Hannover, Germany.
c)Stanford University, 450 Via Palou, Stanford, California 94305-4085.
d)LIGO Laboratory, California Institute of Technology, MS 18-34, Pasadena, California 91125.

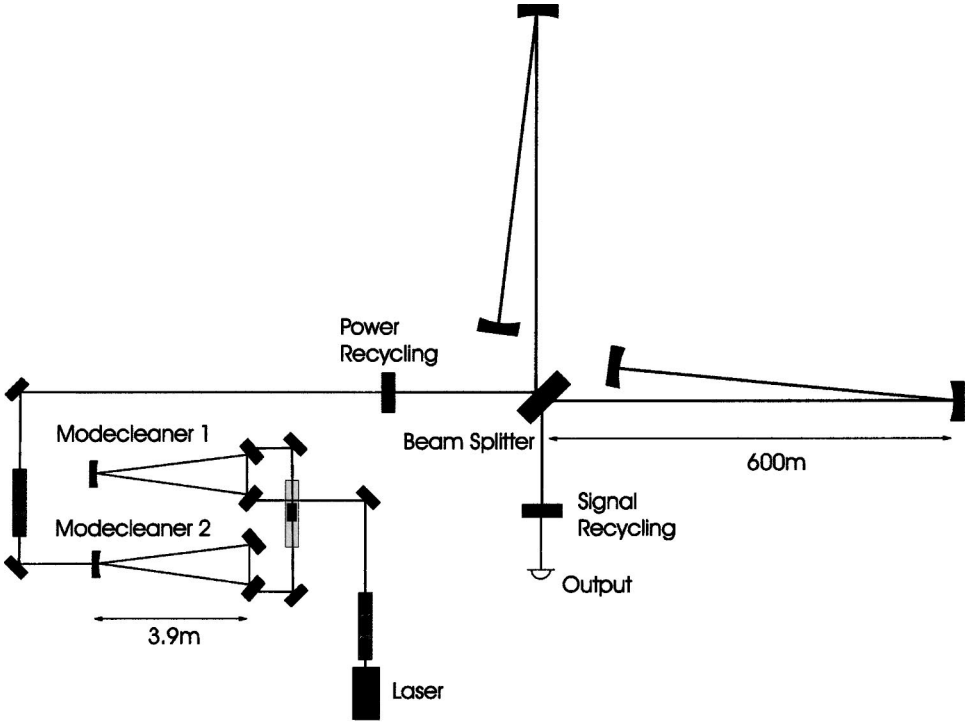

FIG. 1. Simplified optical layout of GEO600. The power-recycling mirror allows maximization of the light power at the beamsplitter, while the signal-recycling mirror controls the frequency response of the detector. The laser beam is spatially and temporally filtered by the two modecleaner cavities (each of 8 m optical pathlength) before being injected into the interferometer. EOMs are located at the laser bench (25.2 MHz, required for the control of the first modecleaner), between the two modecleaners (13 MHz for the second modecleaner and 37.19 MHz for the power-recycling stabilization) and after the second modecleaner (14.9 MHz for the Michelson interferometer and 9 MHz for the signal-recycling stabilization).

quency noise couples into the interferometer output. With a relative arm length asymmetry of $\Delta L/L \simeq 10^{-4}$, the required frequency stability of the light entering the power-recycling cavity is 10^{-4} Hz/$\sqrt{\text{Hz}}$ at 100 Hz.

Due to the finite gain of the control servos, a residual misalignment of the beam splitter, thermal lensing effects in the beam splitter, variations of the index of refractivity inside the beam splitter, a mismatching of the radii of curvature of the mirrors, and asymmetric optical losses in the arms, the interferometer output port cannot be kept perfectly dark. If the fringe offset at the interferometer output port can be kept at $\Delta\Phi = 2\pi \times 10^{-6}$ rad at 100 Hz, the power fluctuations of the light illuminating the power-recycling cavity are allowed to be $5 \times 10^{-8}/\sqrt{\text{Hz}}$ at 100 Hz.[14]

A. Spatial stability

The primary requirement of the modecleaner system is to provide a filter against varying deviations of the laser beam geometry from the power-recycling cavity fundamental Gaussian eigenmode, due to varying contaminations of the fundamental laser mode with higher-order modes.[15] Beam jitter and beam width fluctuations are, due to the mode selectivity of the power-recycling cavity, partly converted into amplitude fluctuations and partly excite higher-order modes within the power-recycling cavity.

From previous measurements,[16] we know that the beam jitter noise δx and beam width noise δw of the Nd:YAG light source, mainly due to varying contaminations of the fundamental TEM_{00} mode with first- and second-order higher modes, respectively, may be as high as

$$\frac{\delta x}{w} \simeq \frac{\delta w}{w} \simeq 10^{-6}/\sqrt{\text{Hz}} \quad \text{at 100 Hz}, \tag{1}$$

where w is the beam width (i.e., the radius).

If the beam splitter is misaligned by 10^{-7} rad, a lateral movement of the laser beam at the beam splitter of $\delta x/w = 10^{-6}/\sqrt{\text{Hz}}$ at 100 Hz would lead to a strain sensitivity limit of the interferometer at 100 Hz of

$$h_{\min} \simeq 7 \times 10^{-18}/\sqrt{\text{Hz}}. \tag{2}$$

Beam width fluctuations of $\delta w/w = 10^{-6}/\sqrt{\text{Hz}}$ at 100 Hz at the beam splitter would cause, due to a mismatching δR of the radii of curvature R of the interferometer mirrors, a strain sensitivity limit at 100 Hz of[17]

$$h_{\min} \simeq 8 \times 10^{-16} \cdot \frac{\delta R}{R}/\sqrt{\text{Hz}}. \tag{3}$$

The specified radii of curvature are 640 m $\pm$ 10 m for the folding mirrors and 600 m $\pm$ 10 m for the end mirrors. This gives a limit at 100 Hz of

$$h_{\min} \simeq 4 \times 10^{-17}/\sqrt{\text{Hz}}. \tag{4}$$

Thus, the illuminating light is required to have less than

$$\delta x/w \leqslant 10^{-11}/\sqrt{\text{Hz}} \tag{5}$$

beam jitter noise and less than

$$\delta w/w \leqslant 10^{-12}/\sqrt{\text{Hz}} \tag{6}$$

beam width noise at 100 Hz at the beam splitter.

This restriction keeps the strain sensitivity limit set by the beam-width noise and beam-position noise well below the limit set by the internal thermal noise of the interferometer optics.

The suppression of higher-order modes of a cavity scales with its finesse $\mathcal{F}$ and largely depends on the cavity geometry.[15] The geometry of the power-recycling cavity is defined by the optical pathlength of 2400 m, the radii of curvature of the interferometer mirrors of 600 m and 640 m,

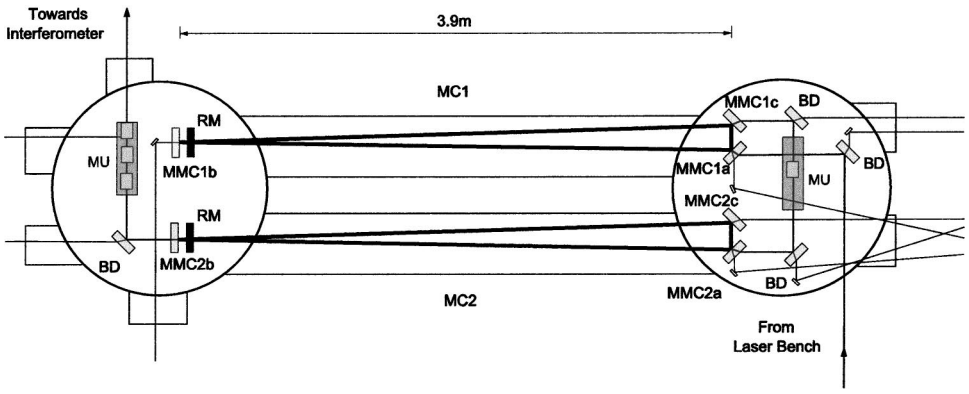

FIG. 2. Optical layout of the modecleaner system. In addition to the six cavity mirrors (MMC1a, MMC1b, ...) four beam-steering (BDs) mirrors are suspended, one each at the input and output of each modecleaner cavity. Two reaction masses (RMs) are suspended in front of MMC1b and MMC2b, to allow length control of the cavities. The EOMs for the second modecleaner and for the interferometer are mounted on suspended platforms, called "mounting units (MUs)," after the first and after the second modecleaner. In addition to the modulators, the last mounting unit supports two Faraday isolators and a lens. Small pick-off mirrors (most have been omitted for clarity here) are mounted on the bottom plates of the vacuum chambers to direct the laser beams needed for the control of the cavities towards the photodiodes (not shown here) that are installed outside the vacuum system.

respectively, and the flat power-recycling mirror. That leads, together with the designed finesse of approximately 4500, to an additional amplitude suppression of about three orders of magnitude for the first higher-order modes. Thus, the modecleaners should provide about four orders of magnitude suppression to give a sufficient safety margin.

Figure 2 shows the optical layout of the GEO600 modecleaner system: Each modecleaner cavity consists of two flat mirrors close together, defining the short side of the triangle and one curved mirror approximately 4 m distant at the acute angle of the triangle. With that geometry, a simplified expression for the suppression factor S_{mn} for the TEM_{mn} mode, is given by

$$S_{mn} \simeq \sqrt{1+4\frac{\mathcal{F}^2}{\pi^2}\sin^2\left[(n+m)\arccos\sqrt{1-\frac{L}{2R}}\right]}, \quad (7)$$

where L is the optical pathlength of the cavity, R is the radius of curvature of the nonplanar mirror, and m,n are integer numbers. For the first and the second modecleaner, the ratio $L/2R$ was chosen to be 0.59 or 0.60, respectively. This ratio provides a significant suppression not only of the TEM_{01} and the TEM_{02} modes to which beam jitter and beam width noise most strongly couple, but also of the next few higher-order modes.

The amplitude suppression factor for one cavity for the first two higher-order modes is

$$S_{01}=S_{10}\simeq S_{02}=S_{20}\simeq 0.49\cdot\mathcal{F}. \quad (8)$$

Thus, the required suppression factor of four orders of magnitude cannot be achieved using a single cavity—the finesse would have to be so high that the throughput would be considerably reduced due to the presence of the finite absorption and scattering losses at the mirrors. For this reason, two mode cleaning cavities are used, yielding other advantages discussed next. Table I shows the calculated suppression factors for the first four higher-order modes of the modecleaners and the resulting suppression factor for the whole system.

B. Temporal stability

The modecleaner system also provides temporal filtering of the transmitted light. Short-term frequency and power fluctuations are reduced by the averaging effect of the optical cavities. The filtering effect is most important at the Fourier frequencies corresponding to the phase modulation sidebands that are applied in order to provide readout of the signals that are required to control the GEO600 interferometer and that contain the interferometer measurement data. The modulation frequencies are in the 8 to 40 MHz range. The extent of the filtering at a given Fourier frequency is determined by the linewidth of the optical resonances of the modecleaners (i.e., the free spectral range divided by the finesse). However, no temporal filtering will occur at Fourier frequencies corresponding to multiples of the free spectral range of the cavities. Hence, the two modecleaners in GEO600 were chosen to be of slightly different round-trip pathlengths of 8.00 m and 8.10 m. Thus, at Fourier frequencies where one modecleaner has a gap in its filtering, the other provides significant filtering. The small length difference should also improve the rejection of very high-order spatial modes that may be present in the ingoing laser beam profile. Identical modecleaners would transmit some higher-order modes that happen to be on resonance, while with slightly different lengths, only some extremely high-order, and hence insignificant, modes are likely to be transmitted through both cavities.

Other requirements of the modecleaners are reliability and autonomous operation, because GEO600 is designed for remote operation with only infrequent human intervention.

TABLE I. Calculated suppression factors of the two modecleaners for the first four higher-order modes.

	TEM_{01}	TEM_{02}	TEM_{03}	TEM_{04}
MC1	1325	1687	822	641
MC2	937	1185	562	474
Overall	1.2×10^6	2×10^6	4.6×10^5	3×10^5

Thus, the duty cycle of the modecleaners should be as close as possible to 100%.

Due to the fact that the seismic noise roughly has the form of 10^{-7} m/$\sqrt{\text{Hz}}\cdot(1\text{ Hz}/f)^2$ above 10 Hz at the detector site, the modecleaners need to be seismically isolated. The mirror motion should not exceed a limit of $\delta x \simeq 6.3 \times 10^{-15}$ m/$\sqrt{\text{Hz}}$ at 100 Hz, set by the Doppler-induced frequency shift of the light.

III. OPTICAL SETUP

The light source for GEO600 is a 14 W injection locked master–slave system with a 1 W Nd:YAG nonplanar ring oscillator (NPRO) as the master laser.[18] The slave laser is a ring oscillator in bow-tie configuration, housed in an Invar spacer. The active media are two Nd:YAG rods, each diode pumped from one end. At low Fourier frequencies, up to 0.5 Hz, the frequency of the master laser is controlled by a thermal drive to maintain resonance with the modecleaners. A piezoelectric actuator controls the emission frequency of the NPRO via stress-induced birefringence in the laser crystal, with a bandwidth of 20 kHz. Up to 100 kHz, the light is kept on the resonance frequency of the cavity with a Li:NbO_3 electro-optic modulator (EOM) as a fast phase shifter.

The mode-matching telescope for the first modecleaner as well as an electro-optic modulator that provides a phase modulation at 25.2 MHz to the laser frequency, required for the length control of the first modecleaner, is located on the laser bench.

The modecleaners were selected to be triangular ring cavities to provide reasonable isolation of the laser system from the returning light. Referring to Fig. 2, the incoming light is coupled into the first cavity (MC1) through the flat mirror MMC1a (**M**irror **M**ode**C**leaner 1 a) and coupled out through the second flat mirror MMC1c. After the first modecleaner, the light is passed through another EOM, providing two phase modulation frequencies at 13 MHz and at 37.197 MHz that are required for the length control of the second modecleaner and for the control of the power-recycling cavity. This modulator is mounted on a suspended platform, a so-called ''mounting unit.'' The light is injected into the second cavity through the flat mirror MMC2a, but, in contrast to the first cavity, coupled out at the acute angle of the triangle through the curved mirror MMC2b. MMC2b has a convex rear surface to form a lens that is the first lens of the mode-matching telescope for the power-recycling cavity. After the second modecleaner, the light is directed toward the interferometer, passing through a third electro-optic modulator, two Faraday isolators, and a second lens. These components are located on the last mounting unit. Some key properties of the two modecleaner cavities are given in Table II, while the optical properties of the cavity mirrors are given in Table III.

For the reasons described herein, the optical pathlengths of the first and second cavity are chosen to be 8.00 m and 8.10 m, respectively, which would lead to a free spectral range (FSR) of 37.48 MHz or 37.02 MHz.

The length of the second modecleaner is tunable by approximately 6 mm with a motor drive, by shifting the position of the suspension point of MMC2b and its reaction pendulum. This drive has not been used so far and is fixed at the short extreme.

TABLE II. Properties of the modecleaner cavities. The optical pathlength, the free spectral range, the beam waist w_0, and the Rayleigh range z_R of each cavity are given.

	MC1	MC2
Optical pathlength	8.00 m	8.10 m
FSR	37.48 MHz	37.12 MHz
w_0	1.05 mm	1.05 mm
z_R	3.3 m	3.3 m

IV. MECHANICAL SETUP

To provide sufficient seismic isolation, each optical component of the modecleaner system (cavity mirrors, beam steering mirrors, and mounting units) is suspended as the lower stage of a double-pendulum (see Fig. 3), described next. Magnet-coil actuators at the intermediate mass allow position and alignment control of each mirror, and provide local damping of the relevant mechanical eigenmodes of the suspensions.

The modecleaner components are housed in two vacuum chambers 1 m in diameter each, connected by two parallel corrugated stainless-steel tubes of 300 mm diameter and 3 m length. Each tube carries the beams for one modecleaner cavity.

An ultrahigh vacuum is used to avoid contamination of the mirrors and to reduce the effect of fluctuations of the refractive index of the air. Furthermore, both acoustic coupling and frictional damping of the suspensions and mirrors are thereby reduced. Only ultrahigh vacuum-safe materials were used, to minimize contamination of the mirrors. The volume of the modecleaner cluster is approximately 4 m^3, pumped by a turbomolecular pump with a pump rate of 180 l/s. The residual gas pressure is 5×10^{-6} Pa (5×10^{-8} mbar), dominated by water vapor.[19]

A. Suspension

Figure 3 shows a schematic drawing of a double-pendulum suspension. The upper suspension wires are attached to a top plate common to all pendulums in one vacuum chamber. This top plate is supported on three two-stage rubber spring isolators, so-called ''stacks.'' These isolators are enclosed in internally damped stainless-steel bellows, to avoid contamination of the vacuum. The design and performance of these isolators has been described in Ref. 13.

TABLE III. Transmission, scattering and the radii of curvature of the modecleaner mirrors as measured by the manufacturer. The four higher transmissive mirrors are used as in- and out-coupling mirrors, respectively.

	Transmission	Scattering	Radius of curvature (front/back)
MMC1a	1778 ppm	23 ppm	flat/flat
MMC1b	35 ppm	35 ppm	concave 6.72 m/flat
MMC1c	1606 ppm	33 ppm	flat/flat
MMC2a	1532 ppm	37 ppm	flat/flat
MMC2b	1360 ppm	28 ppm	concave 6.72 m/convex 0.34 m
MMC2c	114 ppm	32 ppm	flat/flat

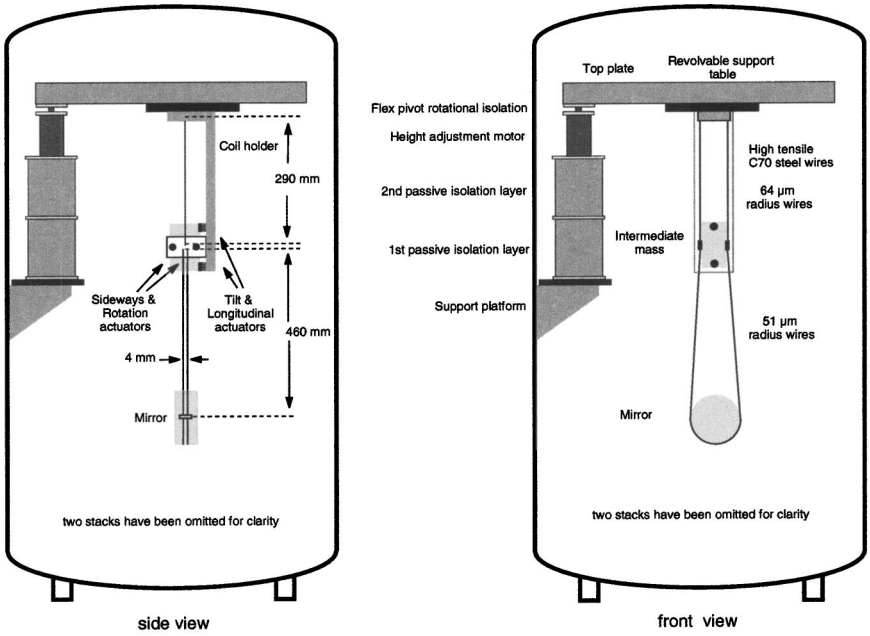

FIG. 3. The suspension scheme of the double pendulums: A mirror, 100 mm in diameter and 50 mm thick, is suspended from an aluminum mass, itself suspended from a support block. Both stages weigh about 0.86 kg. While the mirror lies in two loops made from steel wires, the intermediate mass is suspended by two steel wires, clamped to the mass. The double pendulum itself is hung from a plate that stands on passive isolators. Magnet-coil actuators at the intermediate mass allow alignment control of the pendulums and damping of their fundamental resonances.

For further decoupling of the suspension points from seismic noise, the top plate is connected to the stacks via three ''flex pivots'' that are soft in rotation.

The upper stage of a double pendulum is formed by an aluminum block of about 0.860 kg (the intermediate mass, $85\times75\times50$ mm^3), suspended by two 290 mm long steel wires of 64 μm radius. These wires are clamped to a block at the top plate (the ''slider'') and to the intermediate mass, using small stainless-steel blocks. The four ends of two further steel wires of 51 μm radius are clamped to each intermediate mass to suspend the optics. The upper/lower wires break off the intermediate mass at 5 mm above/below the center of mass. The lower wires form two loops and pass over break-off point defining bars (2 mm above the center of mass) on each side of the cylindrical mirror. The mirrors have a diameter of 100 mm, are 50 mm thick, and weigh 0.864 kg. The lower stage has a length of 460 mm. The first few calculated resonance frequencies of the suspensions are given in Table IV.

To suspend a pendulum the slider, the intermediate mass and a mirror-sized aluminum block are fixed in a ''jig'' that gives the right separations of the masses. Then, the wires are positioned at the masses with a precision of about 0.1 mm, using a positioning jig. This second jig ensures as well that the wires are running rectangular with respect to their clamps, to provide a well defined break-off point without bending of the wires. One end of each wire is then clamped to the intermediate mass. All this is done horizontally on a bench. The other end runs over a pulley and is loaded via a weight to provide similar tension of the two wires within each pendulum stage. While the wires are loaded, the clamps are tightened. The pendulum can then be installed inside the tank without the lowest mass, which is inserted later. The attachment of the suspension to the top plate is done via a revolvable table, allowing the rotational prealignment of the mirrors, while the tilt prealignment is done via a small balancing weight on top of the intermediate mass. The final alignment is done via bias currents through the actuator coils.

The mechanical quality factors Q of the violin modes of the lower stage of a modecleaner pendulum have been measured to be 5×10^5 to 1×10^6.[20]

The control scheme described next necessitates the possibility to apply feedback at one mirror of each cavity. To avoid the coupling of seismic noise to the cavity through the length control actuators, we suspended a reaction pendulum in front of the mirror pendulums MMC1b and MMC2b. This reaction pendulum is made in the same way as the mirror pendulums but instead of a mirror, it contains a reaction mass supporting three coils. The intermediate masses of the reaction pendulum and the mirror pendulum are separated by about 5 mm. With the reaction mass, as well as the mirror, being 35 mm thinner than the intermediate mass, this results in a separation of the lower masses of about 40 mm. The coils protrude from the reaction mass in order to match three magnets (3 mm thick and 10 mm in diameter, made of Nd:Fe:B), bonded onto the surface of the mirror. For these bonds, we used Ceramabond 571 VFG. Since the bonds seem to get weakened under vacuum conditions, we changed to Vacseal for bonding magnets onto the signal-recycling mirror and onto the intermediate reaction masses of the main suspension of the GEO600 interferometer. The reaction

TABLE IV. The calculated values of the relevant resonance frequencies of the double pendulums. Tilt, rotation, and vertical are also known as ''pitch,'' ''yaw,'' and ''bounce,'' respectively. The lower frequencies belong to the common-mode motion of the two pendulum stages, while the higher frequencies are caused by the differential-mode motion of the two stages.

Mode	Resonance frequency (Hz)
Longitudinal and tilt	0.6, 1.3, 1.6, 2.3
Sideways and roll	0.6, 1.5, 15, 34.5
Rotation	0.7, 2.0
Vertical	11.8, 30.1

masses have an aperture of 43 mm in diameter to provide enough clearance for the through going beam.

Furthermore two platforms (mounting units) are suspended as double pendulums using steel wires. Each mounting unit supports an EOM, while one supports in addition to that two Faraday isolators (see Fig. 2).

B. Local control

The position and orientation of the intermediate mass, and as a result of the suspended optics, is controlled in four degrees of freedom using four magnet-coil actuators (see Fig. 3). The Nd:Fe:B magnets (3 mm thick and 10 mm in diameter) are bonded with Ceramabond 571 VFG onto spacers attached to the intermediate mass.[21] The glass-encapsulated coils are mounted on a rigid frame extending down from the top plate.

Simple optical sensors, so-called shadow sensors, are colocated with the actuators. These sense the position of a metal flag bonded onto each magnet, by measuring the degree to which it blocks a beam emitted by an infrared emitter from reaching a silicon photodetector. The sensor components are mounted within the same glass encapsulation as the actuator coil.

The position sensors allow a position/orientation control at low frequencies, and provide a signal that is used for active damping of the relevant mechanical eigenmodes of the suspension. The four sensors and actuators are positioned to sense and control position in the two horizontal degrees of freedom and rotations about the vertical and about the horizontal axis parallel to the reflective surface of a mirror. There is no control in the vertical direction or of roll motion around the normal to the reflective surface of the mirrors.

The control algorithm used to damp the normal modes of the suspension is derived from velocity feedback, optimized for the double-pendulum configuration. The control law used gives better damping of the lowest frequency modes, and includes low-pass filtering to exclude sensor noise above its active band (of approximately 3 Hz). The objective is to provide a short settling time without adding significant noise in the gravitational-wave signal band. This so-called local-control circuit has more than one unity gain frequency, the lowest at 0.3 Hz and the highest at 3 Hz. The fact that there is no gain at very low frequencies allows the application of offset currents to the coils for alignment purposes. The analog local control servo is digitally supervised and can be controlled/adjusted from a personal computer using LABVIEW.[22]

To measure the performance of the local control, we deactivated the damping of a mirror pendulum and applied a step function in the longitudinal direction. After one step, the excitation was turned off and after some seconds of free pendulum oscillation the local control servo was reactivated. The measured performance of the active damping is displayed in Fig. 4. While the quality factor of the undamped motion is in the order $Q \geqslant 10^5$, derived from the measurements of the violin modes, presented in Ref. 20, a quality factor of $Q \simeq 3.5$ is obtained for the damped oscillation.

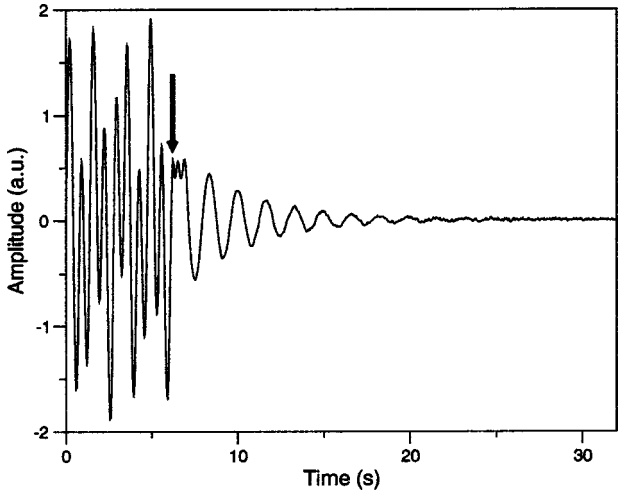

FIG. 4. Performance of the local control by damping the free longitudinal oscillation of a double pendulum. The arrow marks the moment when the damping was activated. A quality factor of 3.5 for the damped oscillation can be calculated from the decay curve.

V. CONTROL TOPOLOGY

Since the control topology is described in detail in Ref. 23, only a brief summary is given here. We use the well known Pound–Drever–Hall sideband technique to stabilize the laser frequency to a resonance of the modecleaner cavities. The laser light is phase modulated at 25.2 MHz to obtain control signals from the light reflected from the first modecleaner. This provides an error signal that is used to control the laser frequency to maintain the light on resonance within the cavity. The laser frequency is thereby defined by the length of the first modecleaner. A second control system, based on a modulation at a frequency of 13 MHz, applied by the second EOM, stabilizes the length of the first modecleaner to the length of the second modecleaner. Thus, the length of the first modecleaner, and hence the laser frequency, is slaved to follow the master second modecleaner. The locking bandwidth of the laser to the first modecleaner is approximately 100 kHz while it is approximately 25 kHz for the first modecleaner to the second.[23] In order to keep the control servos stable, several filter stages, each with a pair of resonant poles and a zero, designed to provide a sharp roll off, are included to avoid exciting internal modes of the mirrors. Finally, the length of the second modecleaner is stabilized to the length of the dual-recycled Michelson interferometer.

During the process of lock acquisition of the first modecleaner, the laser frequency is slowly ramped, since the frequency drift of the free-running laser system would cause the light to be on resonance within the modecleaner cavity only in the order of once per minute. The control loop is closed when the light is resonant in the cavity: If the light power reflected from the first modecleaner falls below a certain threshold, the control system applies feedback to the laser to acquire and extend the lock.

Similarly, the length of the first modecleaner is changed by a step function to minimize the acquisition time of the next control loop which stabilizes the length of the first cavity to the length of the second.

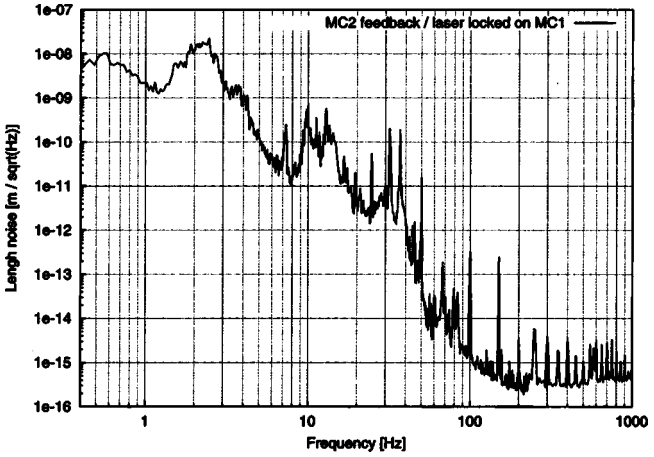

FIG. 5. Differential length noise of the two modecleaners. To record this spectrum the laser was locked to the free hanging first modecleaner, to keep it transparent. Then, the second modecleaner was locked to the first one as well. Displayed is a calibrated feedback spectrum of the second modecleaner.

The stabilization of the master–slave system and of the two modecleaners is fully automated with an average lock acquisition time for the whole system of less than 30 s. The analog control servos are digitally supervised and can be remotely controlled from a personal computer using LABVIEW. The reliability of the system is discussed in Sec. VI.

A further optical technique, the differential wave-front sensing, is used to obtain information about the relative alignment of the beam entering each modecleaner with respect to the fundamental Gaussian laser mode inside each cavity. The signals thus derived are used to control the alignment of the modecleaner mirrors with a bandwidth of 0.2 Hz to ensure maximum throughput of the filtered light. This is described in detail in Ref. 24.

A third phase modulation is needed to provide the Pound–Drever–Hall reflection locking signal for the power-recycling cavity. This modulation at 37.197 MHz is applied between the two modecleaners to benefit from the spatial filtering of the second modecleaner, as well as from temporal filtering. In order to pass it effectively through the second modecleaner, this modulation frequency should be adjusted to be exactly on resonance within this cavity. This is achieved by adjusting the modulation frequency until it corresponds exactly to one free spectral range of the cavity. An optical sensing and control scheme called the ''dc lock'' senses how well this modulation frequency matches the free spectral range of the second modecleaner. This is done by demodulating the light reflected from the second modecleaner at a beat frequency of the two modulation frequencies (13 MHz and 37.197 MHz). Then, the latter modulation frequency can be adjusted to match a free spectral range of the second modecleaner cavity. However, since the long-term drift of the second modecleaner is small enough, the frequency offset needs to be adjusted in the order of only once per month. For simplicity this is done manually, so far. In GEO600, all of the oscillators used to drive EOM are phase locked to a Rb reference oscillator which tracks the global positioning system time standard.

TABLE V. Measured modecleaner quantities. The finesse of the first modecleaner was measured both with a ringdown and an amplitude transfer function method. The finesse of the second modecleaner is derived from the mirror specifications. Furthermore, the measured visibility and throughput of both modecleaners are given.

	First cavity	Second cavity
Finesse	2700	1900
Visibility	94%	92%
Throughput	80%	72%

VI. MEASUREMENTS, RESULTS, AND ANALYSIS

To measure the residual motion of the suspended mirrors, we locked both the laser and the second modecleaner to the first modecleaner. From the feedback signal of the second modecleaner, one gets the differential motion between the two cavities (see Fig. 5).

In the low-frequency regime up to 1 Hz, the spectrum is dominated by seismically induced motion. The bump at 2.3 Hz is caused by the well damped longitudinal and tilt modes of the pendulum. The multiple peak structure at 10 to 12 Hz corresponds to the mechanical resonances of the two tubes connecting the modecleaner vacuum chambers (11.4 and 13.2 Hz) and of the tube that connects the modecleaner vacuum chambers to the power-recycling tank (10 Hz). The tubes are now damped at their centers with styrofoam blocks. The vertical resonance of the double pendulums (common mode at 11.8 Hz) as well as the roll mode at 15 Hz remain undamped. The very narrow peak at 23.5 Hz belongs to a vacuum pump which is now suspended by a coil spring. The two sharp peaks at 31 Hz and 36 Hz are caused by the undamped differential vertical mode of the two pendulum stages and another roll mode, also undamped.

The residual differential motion of the two cavities around 100 Hz is 10^{-15} m/$\sqrt{\text{Hz}}$. This corresponds to a frequency stability of

$$\frac{\delta L}{L}=\frac{\delta\nu}{\nu},\quad \nu\simeq 2.82\times 10^{14}\ \text{Hz}\Rightarrow\ \delta\nu\simeq 30\ \text{mHz}/\sqrt{\text{Hz}}. \tag{9}$$

Finally we locked the length of the second modecleaner to the power-recycled Michelson interferometer which has an optical pathlength of 2400 m.

TABLE VI. Duty cycle of the two modecleaners during an 18 day run. Overall the whole system was in lock for 99.72%, the longest lock lasted for more than 120 h.

Day	1	2–5	6	7	8	9–10	11	12–14	15	16	17	18	**Overall**
MC1 locked (%)	100	100	99.91	99.95	99.98	100	98.86	100	98.82	100	99.62	99.91	**99.84**
MC2 locked (%)	99.98	100	99.87	99.94	99.84	100	98.79	100	97.81	100	99.05	99.76	**99.72**

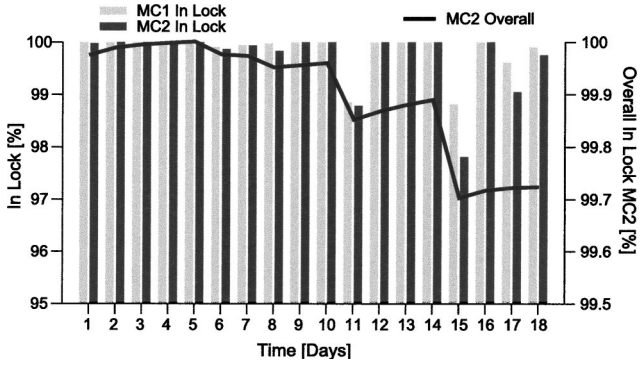

FIG. 6. Long-term measurement of the in-lock time of the modecleaners. The left-hand side axis shows the percentage of in-lock time of each modecleaner per day while the right-hand side axis shows the decay of the overall percentage of the in-lock time of the complete modecleaner system.

Before installing the beam splitter of the Michelson interferometer, we used the power-recycling mirror and one arm of the interferometer as a cavity with an optical pathlength of 2400 m. By doing this the in-loop frequency noise was reduced to 100 μHz/$\sqrt{\text{Hz}}$.[20,22]

The finesse of the first modecleaner cavity was measured both with a ringdown and with an amplitude transfer function method to give the values shown in Table V. Also shown are the measured visibility and throughput of each cavity. The overall throughput of the whole modecleaner system, including all beam steering mirrors, the EOMs and Faraday isolators was measured to be approximately 50%.

A long-term measurement of the in-lock durations was taken in 2002. The power-recycled Michelson interferometer was operated as well at the given time, and since there is a feedback loop from the power-recycling cavity to the length of the second modecleaner, the duty cycle of the modecleaners was influenced by the so far less robust power-recycled interferometer. The obtained statistics are given in Table VI and Fig. 6 for an 18 day period where the percentage of the in-lock durations of both modecleaners was monitored. During that period, the modecleaners fell out of lock seven times and were switched off one additional time to apply adjustments to the servo systems. Examples for the reasons of the lock losses were two earthquakes, a local seismic event, a spike in a laser pump–diode current and a truck passing near by. A typical relock time for the whole system including the slave laser to the master, the master to the first modecleaner, and the first modecleaner to the second one is in the order of 30 s. The longest lock of the whole system achieved in this run lasted for more than 120 h. The overall duty cycle of the whole system during that 18 day period was 99.72%.

ACKNOWLEDGMENTS

This work was supported by PPARC in the UK, the BMBF in Germany, and the state of Lower Saxony.

[1] B. F. Schutz, Class. Quantum Grav. **13**, A219 (1996).
[2] B. F. Schutz, Class. Quantum Grav. **10**, 135 (1993).
[3] K. Danzmann and A. Rüdiger, Rev. Mod. Astron. **15**, 211 (2002).
[4] P. Astone, Class. Quantum Grav. **19**, 1227 (2002).
[5] A. Abramovici, W. E. Althouse, R. W. P. Drever, Y. Gürsel, S. Kawamura, F. J. Raab, D. Shoemaker, L. Sievers, R. E. Spero, K. S. Thorne, R. E. Vogt, R. Weiss, S. E. Whitcomb, and M. E. Zucker, Science **256**, 325 (1992).
[6] C. Bradaschia *et al.*, Nucl. Instrum. Methods Phys. Res. A **289**, 518 (1990).
[7] M. Ando *et al.*, Phys. Rev. Lett. **86**, 3950 (2001).
[8] K. Danzmann and the GEO Team, *Lecture Notes in Physics* (Springer, Berlin, 1992), Vol. 410, p. 184.
[9] B. Willke, P. Aufmuth, C. Aulbert, S. Babak, R. Balasubramanian, B. W. Barr, S. Berukoff, S. Bose, G. Cagnoli, M. M. Casey, D. Churches, D. Clubley, C. N. Colacino, D. R. M. Crooks, C. Cutler, K. Danzmann, R. Davies, R. Dupuis, E. Elliffe, C. Fallnich, A. Freise, S. Goßler, A. Grant, H. Grote, G. Heinzel, A. Heptonstall, M. Heurs, M. Hewitson, J. Hough, O. Jennrich, K. Kawabe, K. Kötter, V. Leonhardt, H. Lück, M. Malec, P. W. McNamara, S. A. McIntosh, K. Mossavi, S. Mohanty, S. Mukherjee, S. Nagano, G. P. Newton, B. J. Owen, D. Palmer, M. A. Papa, M. V. Plissi, V. Quetschke, D. I. Robertson, N. A. Robertson, S. Rowan, A. Rüdiger, B. S. Sathyaprakash, R. Schilling, B. F. Schutz, R. Senior, A. M. Sintes, K. D. Skeldon, P. Sneddon, F. Stief, K. A. Strain, I. Taylor, C. I. Torrie, A. Vecchio, H. Ward, U. Weiland, H. Welling, P. Willams, W. Winkler, G. Woan, and I. Zawischa, Class. Quantum Grav. **19**, 1377 (2002).
[10] H. Lück and the GEO600 Team, Class Quantum Grav. **14**, 1471 (1997).
[11] G. Heinzel, K. A. Strain, J. Mizuno, K. D. Skeldon, B. Willke, W. Winkler, R. Schilling, A. Rüdiger, and K. Danzmann, Phys. Rev. Lett. **81**, 5493 (1998).
[12] M. V. Plissi, K. A. Strain, C. I. Torrie, N. A. Robertson, S. Killbourne, S. Rowan, S. M. Twyford, H. Ward, K. D. Skeldon, and J. Hough, Rev. Sci. Instrum. **69**, 3055 (1998).
[13] M. V. Plissi, C. I. Torrie, M. E. Husman, N. A. Robertson, K. A. Strain, H. Ward, H. Lück, and J. Hough, Rev. Sci. Instrum. **71**, 2539 (2000).
[14] O. S. Brozek, Ph.D. thesis, Universität Hannover, Institut für Atom- und Molekülphysik, 1999.
[15] A. Rüdiger, R. Schilling, L. Schnupp, W. Winkler, H. Billing, and K. Maischberger, Opt. Acta **28**, 641 (1981).
[16] K. D. Skeldon and J. Hough, Rev. Sci. Instrum. **66**, 2760 (1995).
[17] K. D. Skeldon, K. A. Strain, A. I. Grant, and J. Hough, Rev. Sci. Instrum. **67**, 2443 (1996).
[18] I. Zawischa, M. Brendel, K. Danzmann, C. Fallnich, M. Heurs, S. Nagano, V. Quetschke, H. Welling, and B. Willke, Class. Quantum Grav. **19**, 1775 (2002).
[19] H. Lück and the GEO Team, *Gravitational Waves*, edited by E. Coccia, G. Veneziano, and G. Pizzella (World Scientific, Singapore, 1998).
[20] S. Goßler, M. M. Casey, A. Freise, H. Grote, H. Lück, P. McNamara, M. V. Plissi, D. I. Robertson, N. A. Robertson, K. Skeldon, K. A. Strain, C. I. Torrie, H. Ward, B. Willke, J. Hough, and K. Danzmann, Class. Quantum Grav. **19**, 1835 (2002).
[21] To avoid any bonds, we used thin plates made from magnetizable stainless steel to stick the magnets to, for the GEO600 signal-recycling suspension. These plates can be bolted onto aluminum spacers.
[22] M. M. Casey, H. Ward, and D. I. Robertson, Rev. Sci. Instrum. **71**, 3910 (2000).
[23] A. Freise, M. M. Casey, S. Goßler, H. Grote, G. Heinzel, H. Lück, D. I. Robertson, K. A. Strain, H. Ward, B. Willke, J. Hough, and K. Danzmann, Class. Quantum Grav. **19**, 1389 (2002).
[24] H. Grote, G. Heinzel, A. Freise, S. Goßler, B. Willke, H. Lück, H. Ward, M. Casey, K. A. Strain, D. Robertson, J. Hough, and K. Danzmann, Class. Quantum Grav. **19**, 1849 (2002).